MAGNETOHYDRODYNAMICS Vol. 49 (2013), No. 1, pp. 223–229

THE MHD TRAVELLING MAGNETIC FIELD PUMP FOR LIQUID MAGNESIUM

S. Denisov[1], *V. Dolgikh*[1], *R. Khalilov*[1], *I. Kolesnichenko*[1,2], *S. Khripchenko*[1,2]

[1] *Institute of Continuous Media Mechanics, Ural Branch of Russian Academy of Sciences 1 Acad. Korolyeva str., 614061 Perm, Russia e-Mail: khalilov@icmm.ru*

[2] *Perm National Research Polytechnic University, Perm, Russia*

In this work, we consider an MHD pump generating a travelling magnetic field. It consists of six C-shaped inductors located one after another. A flat channel for pumping liquid metal is placed in the gap between the inductors. The cores are fed by the alternating current from a three-phase source and are connected in such a way as to provide the generation of a travelling wave. Due to the pump design, the electrical windings in such a pump are located at a safe distance from the heated channel with liquid metal. The channel can be quickly removed and placed back into the pump. The paper presents results of experimental and numerical investigations of the temperature regimes and numerical simulation of magnetic fields in the ferromagnetic cores of the pump inductor. Numerical computation has been done to evaluate the electromagnetic volume forces, acting on the transporting channel. The pressure drop–flow rate characteristics of the pump have been obtained for a gallium circuit. The workability of the pump has been tested in liquid magnesium.

1. Introduction. With various induction-type MHD equipment, the machines with linear flat and cylindrical channels are in most common use. They are known as the induction electromagnetic pumps with a travelling magnetic field (TMF) generated by a three-phase alternating current system. The operation of such pumps is based on the following principle: a three-phase winding located in the inductor slots generates a travelling magnetic field, which induces an electric current in the layer of liquid metal. The interaction of these currents with the resultant magnetic field generates electromagnetic forces directed along the travelling magnetic field.

Application of the TMF pumps in the non-ferrous metal casting industry has some restrictions, which are mainly due to the design peculiarities of these pumps. Indeed, in the case of traditional design, the electric windings of such pumps are found to be in the immediate vicinity of a strongly heated channel, which leads to their overheating and eventually to rapid failure. Thus, for example, in the TMF pump used for casting large-size magnesium ingots, the electric windings are the most frequently replaced part of the pump because, due to the extremely high temperature regime, they fail very quickly. On the other hand, the TMF pump has a straight channel of elementary configuration and can be easily and quickly made from a metal tube (as it is usually done for liquid magnesium and similar metals), which is certainly an obvious advantage of these pumps in contrast to other pump types [1].

2. Numerical calculations of electromagnetic fields. To simulate numerically the inductor of the TMF pump, it is necessary to calculate the magnetic

(*a*)

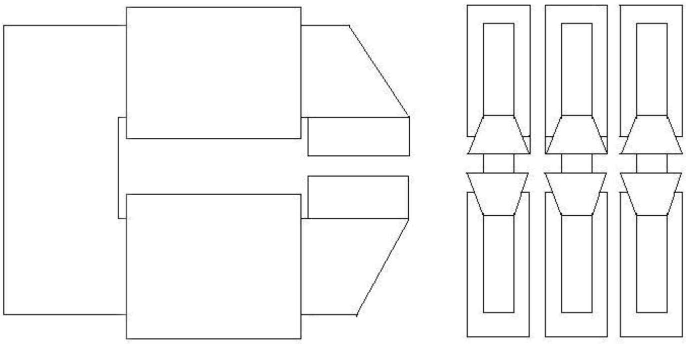

(*b*)

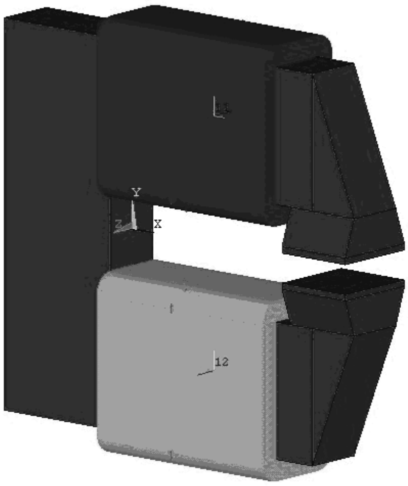

Fig. 1. Left: schematic of the computational model including three inductors; right: inductor with bias coils. (*a*) (*b*)

field distribution. Such numerical calculations are essential for revealing the regions, in which the value of the magnetic field induction will be high enough. With this approach, in the inductor gap of rather small size, a magnetic field of prescribed value can be genetared. Calculations of the electromagnetic fields were carried out using the ANSYS software product and the following computational scheme: a model consisting of three inductors was situlated in a three-dimensional (3D) space. The central inductor incorporates three biasing coils, while the neighbouring inductors are considered passive. The advantage of this approach is that it makes it possible to take into account the dissipation of the magnetic field by closing the magnetic field travelling through the neighbouring passive inductors (Fig. 1).

To fit the geometrical parameters of the model and to simplify the calculations, we used two symmetry planes. The magnetic fields inside the inductor were calculated based on the non-linear characteristics of B-H magnetization. The results of these calculations of the magnetic field distribution inside the inductor are shown in Fig. 2 (the results are presented for 1/4 part of the model).

The non-linear characteristics of B-H magnetization used for calculations allowed us to reveal “weak” zones of the inductor (Fig. 2), which are most liable to magnetic saturation (red zones with a magnetic field value of about 1.8 T). Note that the value of the magnetic field in the gap of the inductor is a parameter,

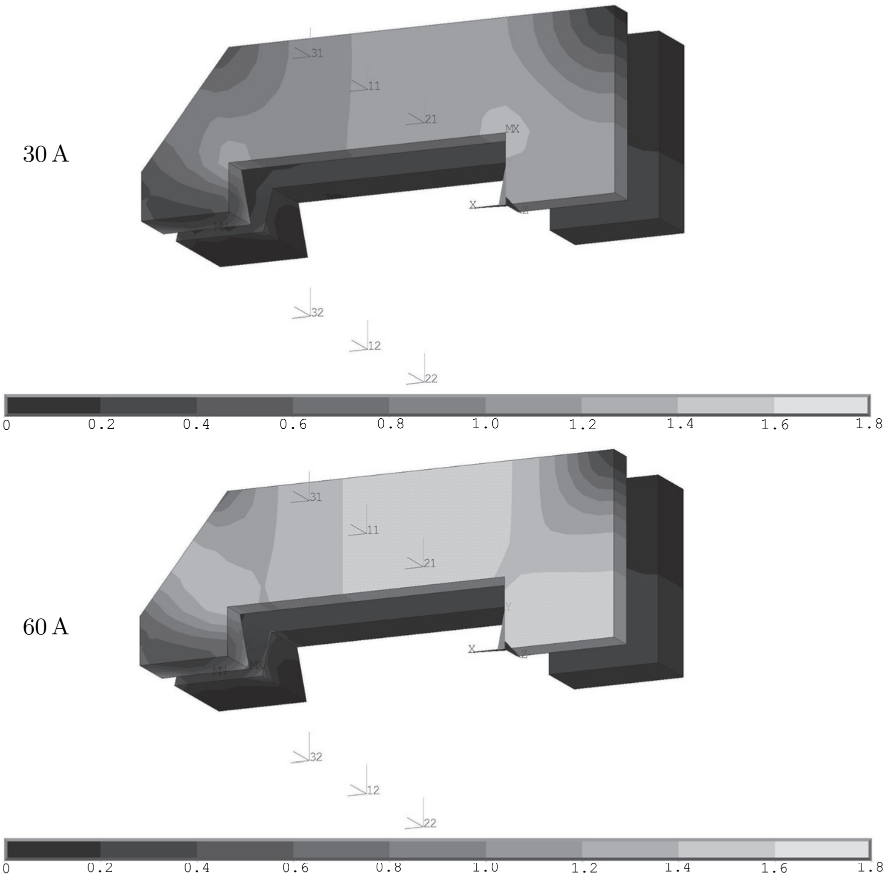

Fig. 2. Magnetic field inside the inductor for the values of bias coil current 30 and 60 A (the range corresponds to 0–1.8).

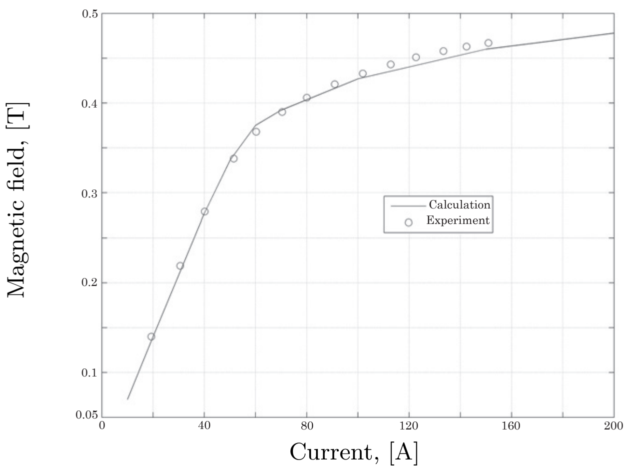

Fig. 3. The magnetic field intensity versus the values of bias coil current (measurement error is about 2%).

which is also essential for primary estimation of the characteristics of the TMF pump (Fig. 3). To have deeper insight into the interaction between the electromagnetic fields in the inductors of the TMF pump, magnetic field simulations were made for a variety of geometrical parameters. In particular, in the course of calculations, we varied the size of the non-magnetic gap of the inductor (30 mm and 35 mm) and the thickness of the inductor (from 70 mm to 110 mm). The results show that the magnetic field in the gap increases with the inductor thickness. This can be explained by an increase in inductor volume, which leads to a decrease in saturation threshold, i.e. to a significant reduction of the magnetic field dissipation. The decrease in width of the non-magnetic gap has the same positive effect.

3. Hydrodynamic calculations. We consider a plane fluid layer (liquid metal) bounded by solid walls. The planar dimension of such a channel is much greater than its thickness. The liquid metal in the channel is under the action of the volume electromagnetic forces. The flow driven in the channel can be of a transitional pattern.

The fluid flow in a plane channel under the action of electromagnetic forces is described by the Navier–Stokes equations. Here, the inductionless approximation is fulfilled provided that the velocity of the metal flow is low. Therefore, the inverse effect of the flow on the magnetic field is neglected.

Thus, the velocity field of turbulent flow in a plane channel was defined using the above-mentioned approximate equations. Numerical simulations were carried out using the correlated scheme for velocity and pressure. The partial differential equations were approximated by applying the conservative schemes of the finite-difference method. Boundary conditions for vorticity were calculated using the internal iteration method.

We have calculated patterns of the flow in the pump channel (Fig. 4). The obtained results suggest that the interaction of the electromagnetic forces initiates an irregular vortex flow in the channel responsible for the appearance of pressure pulsations generated by the pump. The calculated average amplitude of the pulsations was of order of 5% of the full value of the pressure developed by the pump.

4. Heat calculations. Under the operation conditions, different elements of the pump release heat. We consider a flow of liquid magnesium through a flat MHD channel placed between the core poles. The channel is heated to 670°C and, in spite of thermal insulation, transfers heat to the pump's cores that causes heating of the pump elements. Besides, heat is also generated in the pump coils, through which the electric current passes. The temperature of some elements may reach values exceeding the threshold values of thermal resistance of the materials used for constructing the pump units. Therefore, we performed physical experiments with a physical model of the pump and made thermal calculations for a supposed pump structure. The purpose of those calculations was to design a pump such that the temperature of its separate elements during operation did not exceed an ultimate thermal resistance of the materials used for constructing the pump elements.

(*a*)

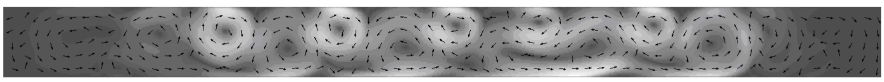

(*b*)

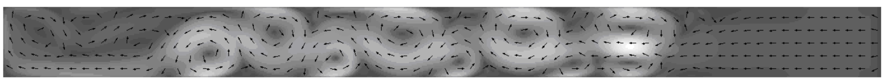

Fig. 4. A flow pattern in the pump channel: *a*) zero flow regime, $B = 0.09$ T; (*b*) operation regime, $B = 0.19$ T, $q = 200$ ml/s.

The temperature fields in the elements of the MHD pump were determined by solving numerically the equations of heat flow generated by corresponding sources. To this end, we set the conditions of heat release described by the corresponding approximate heat transfer equations on the external surfaces of the pump elements:

$$q = \alpha(T_{\text{w}} - T_{\text{air}}), \tag{1}$$

where T_{w} is the temperature of a heated wall, T_{air} is the temperature of the surrounding air or a cooling flux.

On the external surface, from which the heat is released into the environment due to free convection, the heat transfer coefficient α is calculated by an approximate formula

$$\alpha = 1.77(T_{\text{w}} - T_{air})^{0.33}. \tag{2}$$

On the surface, where the heat release is caused by forced-air cooling, the heat transfer coefficient α is calculated by an approximate formula

$$\alpha = \frac{0.032\lambda_{\text{air}}}{L}\left(\frac{L}{\nu_{\text{air}}}\right)^{0.8} V^{0.8}. \tag{3}$$

Here L is the length of the heat transfer area, V is the rate of the cooling air flux, ν_{air} and λ_{air} are the kinematic viscosity and thermal conductivity of the air, respectively.

To stimulate calculations, we considered the symmetry of the pump and performed calculations only for 1/4 part of the designed structure.

5. Physical experiment with gallium. The pump was tested with a gallium unit, through which the gallium alloy (Ga 87.5%; Sn 10.5%; Zn 2%) was pumped. The purpose of the test was to determine the flow rate–pressure drop characteristics of the pump at different values of the phase current.

During the experiment, a three-phase current was controlled by a special power supply source suggesting partial compensation of the reactive power of the pump. The pressure generated by the pump was measured using the METPAH measuring system, and the flow rate of the gallium alloy was measured by a conduction-type flowmeter designed and manufactured by the authors of this paper.

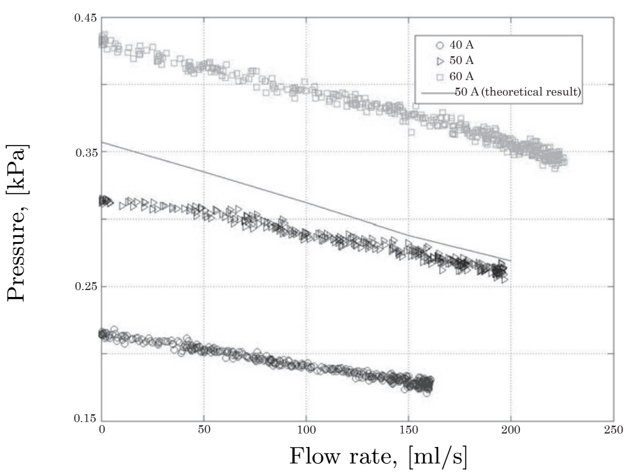

Fig. 5. Pump characteristics: flowrate–pressure drop characteristics.

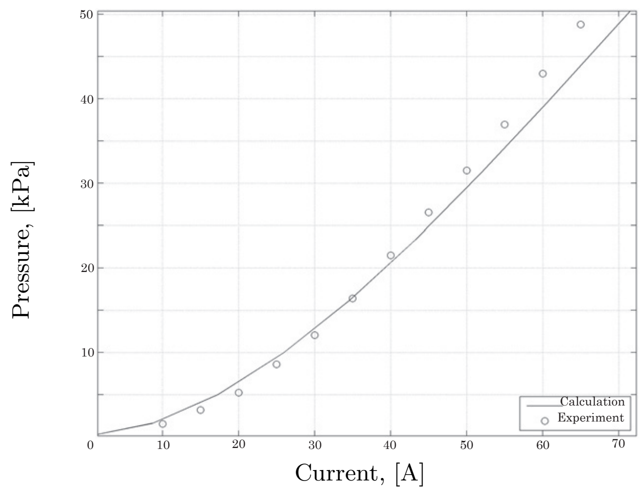

Fig. 6. Pump characteristics: pressure under zero flow conditions (measurement error is about 5%).

The results of the measurements were used to evaluate the flow rate–pressure drop characteristics of the pump driven by the three-phase current (Fig. 5), and the dependence of the maximum pressure difference in the case of zero flowrate on the phase current value (Fig. 6).

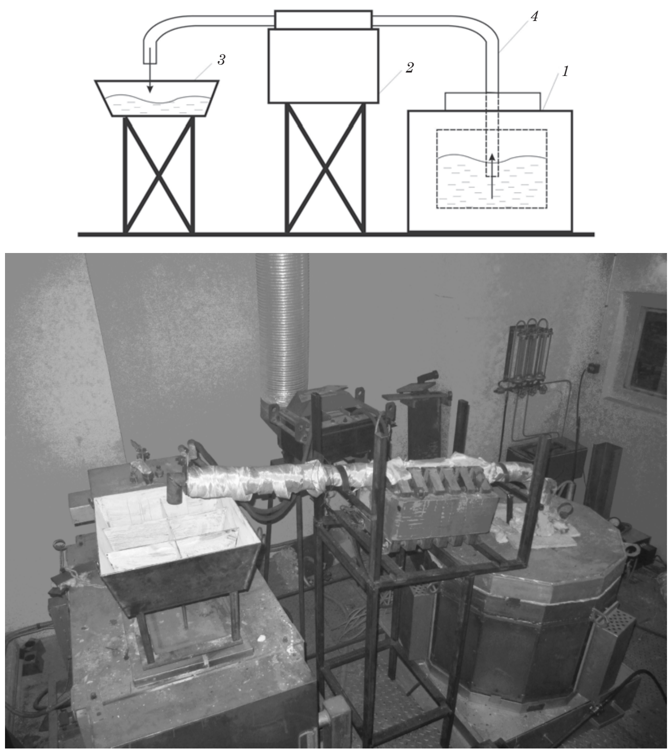

Fig. 7. Schematics and picture of the experimental setup for testing the liquid magnesium pump.

6. Physical experiment with liquid magnesium. The MHD pump was also tested in a setup filled with liquid magnesium. For this purpose, the pump was mounted on a special supporting base near a crucible furnace for liquid magnesium (Fig. 7). The tests showed that the pump transporting the magnesium from the crucible to the receiving reservoir demonstrated good performance. In the beginning of discharge, at a value of the phase current of 50 A, the pump lifted magnesium to a height of 1.2 m and at the end of discharge, at a height of 1.4 m, the average flowrate was 1.32 kg/s. Because of the complexity and time-consuming preparations the experiment was not repeated and the scatter in values of the mean flow rate was not determined.

Acknowledgements.
The work was supported by RFBR grant no. 11-08-00416-a.

REFERENCES

[1] S. Khripchenko, R. Khalilov, I. Kolesnichenko, S. Denisov, V. Galindo, G. Gerbeth. Numerical and experimental modelling of various MHD induction pumps. *Magnetohydrodynamics*, vol. 46 (2010), no. 1, pp. 85–97.

Received 03.11.2012